Current Science
CS 5 (3), 3045-3058 (2025)
Received 23 March 2025 | **Revised 22 April** 2025 | **Accepted 21 May**. 2025 | **Online Available 16 June** 2025
https://doi.org/ 10.52845/CS/2025-5-3-74

Current Science

Current Science

OPEN ACCESS

ISSN (O) 2795-8639

Original Article

Three-Dimensional Vibration Analysis of Fiber-Plain-Woven Composite Beams with General Boundary Conditions

Jing Peng[a*], Linghong Guo[a], Bihua Du[a], Zishan He[a]

[a]Chengdu Textile College, Chengdu, 611731, China

[*]Corresponding Author: Jing Peng

Abstract:
A three-dimensional differential quadrature model is developed to study the free vibration of fiber plane-woven composite beams with arbitrary combinations of boundary conditions. The fiber-plain-woven composite material is assumed to be a three-dimensional orthotropic anisotropic material. The vibration model for the fiber-plain-woven composite beam is formulated by the three-dimensional elasticity theory combined with the differential quadrature method (DQM), where various boundary conditions (including free, clamped, simply-supported as well as elastic constraints etc.) are flexibly simulated by boundary springs with variable stiffness. In order to clarify the accuracy of the developed model and methodology, some free vibration solutions for isotropic, composite beams in different boundary combinations of free, simply-supported, clamped and elastic constraints are given, where the current solutions are in good agreement with the literature solutions and finite element numerical results. After that, some parameter investigations are carried out to explore the impact of boundary stiffness, volume fraction and geometric dimensions on the vibration properties. Additionally, the obtained new benchmark solutions for fiber-plain-woven composite beams may be used to check the accuracy of other simplified beam theories.
Keywords: Vibration characteristics; fiber-plain-woven material; 3D beams; general boundary conditions.

1. Introduction

The dynamic modeling of beam structures plays a critical role in engineering practice. By mathematically characterizing their behavior under dynamic loads (e.g., vibrations, impacts, or cyclic forces), it enables the prediction of structural responses, prevention of resonance failures, and optimization of vibration control strategies. Furthermore, it provides essential guidance for fatigue resistance design, safety assessment, and performance enhancement in fields such as bridge engineering, civil construction, and aerospace applications, ultimately ensuring structural reliability, durability, and cost-effectiveness. Current research predominantly simplifies three-dimensional elasticity problems into one-dimensional formulations by introducing various assumptions [1-3]. While this approach significantly improves computational efficiency, it proves inadequate for scenarios involving large deformations, geometric nonlinearities, and complex boundary conditions. Consequently, researchers have developed advanced modeling techniques for three-dimensional beam dynamics. Contemporary studies not only encompass experimental validation [4-7] but have also pioneered numerical methodologies including: Finite element methods [8-12], Modal Analysis methods [13-16], Isogeometric analysis [17-24] and so on. Jonker [25] developed a three-dimensional beam element based on the generalized strain beam formulation to investigate the stability of elastic thin-walled open-section beams in multibody systems. Nguyen et al. [26] developed a geometrically nonlinear dynamic model for three-dimensional beam structures using the Lagrangian description, and applied it to

analyze large deformation behaviors of both straight and curved beams under various loading conditions. Huang et al. [27] proposed a modified smoothed particle method for effectively analyzing the quasi-static and dynamic behaviors of three-dimensional Timoshenko beams with geometric nonlinearity. Nguyen et al. [28] developed a three-dimensional beam analysis model within the isogeometric analysis framework, successfully resolving large-deflection responses of functionally graded curved beams. Based on three-dimensional linear elasticity theory, Qu et al.[29] employed the variational principles and a multi-segment modeling strategy develop a 3D model of a composite rectangular parallelepipeds, and analyzed the free and transient vibration characteristics of the beams, plates as well as solids. For the vibration problems of beam having variable thickness cross-section, Chen et al.[30] presented a three-dimensional isogeometric vibration model considering axial functionally graded materials, and investigated the impact of some parameters, such as geometrical proprieties, boundary conditions, etc, on the vibration behaviors of the beam.

Engineering structures fabricated from woven composites have found extensive applications in marine and aerospace engineering due to their superior strength-to-weight ratios and high specific stiffness [31]. Considerable research efforts have been devoted to developing predictive models for the mechanical properties of these woven composite materials. Nicoletto et al. [32] investigated the mechanical behavior of woven fiber composites through an integrated approach combining experimental characterization and finite element simulations. Liu et al. [33, 34] developed an extended mechanics of structure genome approach for effective prediction of the thermoelastic behavior of woven fiber composites. Adumitroaie et al. [35] developed a generalized three-dimensional analytical model to investigate the mechanical properties of woven fiber composites. Based on the simplified beam and plate theory, Zhang et al.[36] used the differential quadrature finite element method (called DQFEM) to derive dynamic equations of fiber-woven shaft–disk rotor system with different shapes of holes and investigate the material parameters and hole parameters on its dynamic behaviors. Tan et al. [37-39] employed finite element modeling to predict the mechanical properties and failure strength of woven fiber composites. Zhang et al. [40] developed a simplified finite element-based model to analyze the micromechanical behavior of woven fiber composites. Huang et al.[41] applied the called first order shear deformation theory in conjunction with generalized differential quadrature approach to analyze the free vibration properties of a conical-cylindrical combined shell made of carbon-fiber plain woven reinforced composite, in which the thermal environment was considered.

A comprehensive literature review reveals substantial research achievements in both three-dimensional beam dynamics modeling and mechanical property prediction of woven fiber composites. However, studies specifically addressing three-dimensional beams composed of plain-woven composites remain notably scarce. To address this research gap, the present work establishes a free vibration analysis model for 3D plain-woven composite beams under arbitrary boundary conditions. Within the unified framework combining three-dimensional elasticity theory and the differential quadrature method (DQM), the plain-woven composite is equivalently treated as a 3D orthotropic material, while boundary spring technology is employed to simulate various constraint conditions. The validity of the proposed 3D-DQM model is verified through comparative analyses with existing analytical solutions and finite element results. Furthermore, parametric studies systematically investigate the influence of boundary constraints, material parameters, and geometric dimensions on the vibrational characteristics of plain-woven composite beams.

2. Mathematical Formulations

The physical model and the associated coordinate system of the 3D beam with rectangular cross-section are displayed in Fig.1, and the symbols L, B and H denote the length, width and thickness of the beam, respectively. The beam is made of a linear elastic three-dimensional fiber-plain-woven material and it is assumed that the main axis of the material is oriented in the same direction as the axes of the adopted coordinate system. The displacement components along the x-, y-, and z-axes at any point in the beam are denoted as u, v, and w, respectively, which are functions of the spatial coordinates (x, y, z) and the time variable t.

Note that only the surfaces at x = 0, L can be subjected to arbitrary types of boundary conditions in the present study, while others surfaces are assumed to be stress free.

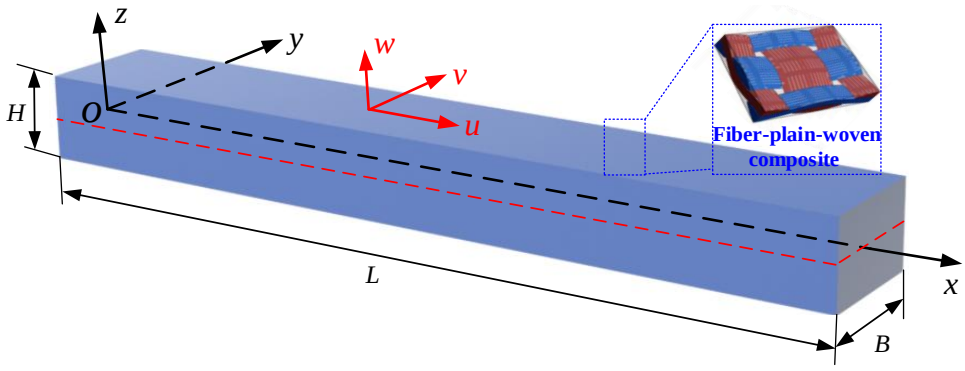

Figure 1: Geometric dimensions and co-ordinate system of a fiber-plain-woven composite 3D beam

2.1. Material Model

Fiber woven reinforced composites refer to a class of advanced materials consisting of fiber woven preforms as the reinforcing phase and polymer/metal/ceramic matrices, which are consolidated through curing processes to form integrated composite systems. In this paper, the widely used carbon fiber orthogonal plain woven reinforced resin matrix composites are selected, whose material properties at different fiber volume fractions are shown in Fig. 2 (See Ref.[36, 41] for the detailed descriptions). Of note, the symbols E_{11}, E_{22} and E_{33} given in Fig.2 are used to represent the Young's modulus in the principal directions, when the shear moduli are denoted by G_{12}, G_{23} and G_{13}. In addition, the symbols μ_{12}, μ_{13} and μ_{23} are the Poisson's ratios and ρ is the mass density. Here, the curves with the same color as the vertical axis use that axis scale and label. For example, the 2D curves corresponding to E_{11}, E_{22} and E_{33} share the blue axis in Fig.2(a), while the ones related to G_{12}, G_{23} and G_{13} use the pink axis. It should be pointed out that fiber-plain-woven composite can be considered as a special orthotropic anisotropic material. In terms of isotropic beam, the corresponding engineering constants are set as: $E_{11}=E_{22}=E_{33}=E$, $\mu_{12}=\mu_{13}=\mu_{23}=\mu$ and $G_{12}=G_{23}=G_{13}= E/[2(1+\mu)]$.

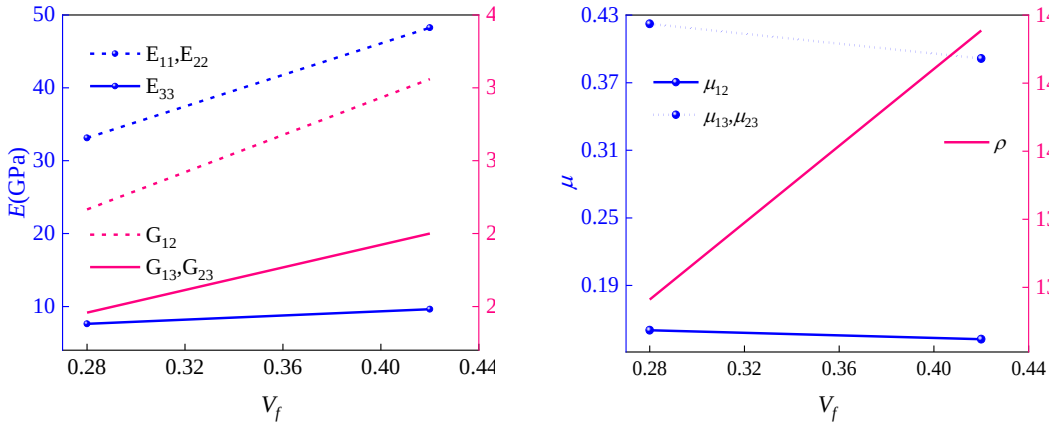

(a) Young's modulus and shear modulus (b) Density and Poisson's ratio

Figure 2: Material parameters of fiber-plain-woven composite with different volume fractions V_f

2.2. Displacement Field and Kinematic Relations

According to the three-dimensional theory of elasticity, within the linear elastic regime, the kinematic relations of an elastic body can be expressed in vector form as

$$\boldsymbol{\varepsilon} = \left\{ \varepsilon_x \quad \varepsilon_y \quad \varepsilon_z \quad \varepsilon_{xy} \quad \varepsilon_{xz} \quad \varepsilon_{yz} \right\}^{\mathrm{T}} = \mathbf{E}_1 \mathbf{U} \qquad (1)$$

where $\mathbf{E}_1$ and $\mathbf{U}$ are

$$\mathbf{E}_1 = \begin{bmatrix} \frac{\partial}{\partial x} & 0 & 0 & \frac{\partial}{\partial y} & \frac{\partial}{\partial z} & 0 \\ 0 & \frac{\partial}{\partial y} & 0 & \frac{\partial}{\partial x} & 0 & \frac{\partial}{\partial z} \\ 0 & 0 & \frac{\partial}{\partial z} & 0 & \frac{\partial}{\partial x} & \frac{\partial}{\partial y} \end{bmatrix}^{\mathrm{T}}, \mathbf{U} = \begin{bmatrix} u \\ v \\ w \end{bmatrix} \tag{2}$$

Based on the generalized Hooke's law, the constitutive equations of a linear elastic body can be defined as:

$$\begin{Bmatrix} \sigma_x \\ \sigma_y \\ \sigma_z \\ \sigma_{yz} \\ \sigma_{xz} \\ \sigma_{xy} \end{Bmatrix} = \begin{bmatrix} C_{11} & C_{12} & C_{13} & 0 & 0 & 0 \\ C_{12} & C_{22} & C_{23} & 0 & 0 & 0 \\ C_{13} & C_{23} & C_{33} & 0 & 0 & 0 \\ 0 & 0 & 0 & C_{44} & 0 & 0 \\ 0 & 0 & 0 & 0 & C_{55} & 0 \\ 0 & 0 & 0 & 0 & 0 & C_{66} \end{bmatrix} \begin{Bmatrix} \varepsilon_x \\ \varepsilon_y \\ \varepsilon_z \\ \varepsilon_{yz} \\ \varepsilon_{xz} \\ \varepsilon_{xy} \end{Bmatrix} \tag{3}$$

in which the elastic modulus C_{ij} (i, j=1, 2, 3, 4, 5, 6) appeared in Eq. (3) is given by

$$\begin{aligned} &C_{11} = E_{11}\frac{1-\mu_{23}\mu_{32}}{\Delta}, C_{12} = E_{11}\frac{\mu_{21}+\mu_{31}\mu_{23}}{\Delta}, C_{13} = E_{11}\frac{\mu_{31}+\mu_{21}\mu_{32}}{\Delta} \\ &C_{22} = E_{22}\frac{1-\mu_{31}\mu_{13}}{\Delta}, C_{23} = E_{22}\frac{\mu_{32}+\mu_{12}\mu_{31}}{\Delta}, C_{33} = E_{33}\frac{1-\mu_{12}\mu_{21}}{\Delta} \\ &C_{44} = G_{23}, C_{55} = G_{13}, C_{66} = G_{12} \\ &\Delta = 1-\mu_{12}\mu_{21}-\mu_{23}\mu_{32}-\mu_{31}\mu_{13}-2\mu_{21}\mu_{32}\mu_{31} \\ &\mu_{21} = \frac{E_{22}}{E_{11}}\mu_{12}, \mu_{32} = \frac{E_{33}}{E_{22}}\mu_{23}, \mu_{31} = \frac{E_{33}}{E_{11}}\mu_{13} \end{aligned} \tag{4}$$

Rearranging the above constitutive relations, the vector form of Eq. (3) can be represented as follows

$$\boldsymbol{\sigma} = \begin{Bmatrix} \sigma_x & \sigma_y & \sigma_z & \sigma_{xy} & \sigma_{xz} & \sigma_{yz} \end{Bmatrix}^{\mathrm{T}} = \mathbf{C}\boldsymbol{\varepsilon}$$

$$\mathbf{C} = \begin{bmatrix} \mathbf{C}_1 & \mathbf{0} \\ \mathbf{0} & \mathbf{C}_2 \end{bmatrix}, \mathbf{C}_1 = \begin{bmatrix} C_{11} & C_{12} & C_{13} \\ C_{12} & C_{22} & C_{23} \\ C_{13} & C_{23} & C_{33} \end{bmatrix}, \mathbf{C}_2 = \begin{bmatrix} C_{44} & 0 & 0 \\ 0 & C_{55} & 0 \\ 0 & 0 & C_{66} \end{bmatrix} \tag{5}$$

2.3. Energy functionals

The strain energy of the three-dimensional fiber-plain-woven beam can be stated as

$$U = \frac{1}{2}\int_V \boldsymbol{\varepsilon}^{\mathrm{T}}\boldsymbol{\sigma}\mathrm{d}V = \frac{1}{2}\int_V \boldsymbol{\varepsilon}^{\mathrm{T}}\mathbf{C}\boldsymbol{\varepsilon}\mathrm{d}V = \frac{1}{2}\int_V \left(\mathbf{U}^{\mathrm{T}}\mathbf{E}_1^{\mathrm{T}}\right)\mathbf{C}\left(\mathbf{E}_1\mathbf{U}\right)\mathrm{d}V \tag{6}$$

where V denotes the volume of the beam, which is the integration region of the above equation, and dV=dxdydz.

The kinetic energy of the three-dimensional fiber-plain-woven beam can be described in the form of the displacement vector as follows

$$T = \frac{1}{2}\int_V \rho \dot{\mathbf{U}}^{\mathrm{T}} \dot{\mathbf{U}} \mathrm{d}V \qquad (7)$$

The boundary conditions at the left and right ends of the beam are modeled using three sets of constrained springs, and the additional boundary potential energy thus introduced is expressed as

$$U_{\mathrm{BC}} = \frac{1}{2}\int_V \left[\left(\mathbf{U}^{\mathrm{T}} \mathbf{k}_{\mathrm{B0}} \mathbf{U} \right)\Big|_{x=0} + \left(\mathbf{U}^{\mathrm{T}} \mathbf{k}_{\mathrm{B1}} \mathbf{U} \right)\Big|_{x=L} \right] \mathrm{d}V \qquad (8)$$
$$\mathbf{k}_{\mathrm{B}i} = \mathrm{diag}\left(k_{ui} \quad k_{vi} \quad k_{wi} \right), i = 0, 1$$

in which k_u, k_v and k_w represent the spring stiffness.

Superposition of Eqs. (6) ~ (8) yields the overall energy generalization of the three-dimensional beam structure as follows

$$L = T - U - U_{\mathrm{BC}} \qquad (9)$$

2.4. Vibration solutions

Based on Hamilton's principle, the control equations are obtained by performing variational operations as follows

$$\int_{t_1}^{t_2} \delta L \mathrm{d}t = 0 \qquad (10)$$

i.e.

$$\int_{t_1}^{t_2} \left[\int_V \delta \mathbf{U}^{\mathrm{T}} \rho \ddot{\mathbf{U}} - \delta \mathbf{U}^{\mathrm{T}} \mathbf{E}_1^{\mathrm{T}} \mathbf{C} \mathbf{E}_1 \mathbf{U} - \left(\delta \mathbf{U}^{\mathrm{T}} \mathbf{k}_{\mathrm{B}} \mathbf{U} \right)\Big|_{x=0,L} \mathrm{d}V \right] \mathrm{d}t = 0 \qquad (11)$$

In the basic framework of DQM, the beam structure is meshed in x, y, and z directions into N, M, and P nodes, respectively. The above energy functions are discretized by converting the derivatives of the displacement components into discrete form using differential operators. The discrete form is expressed as follows

$$\int_{t_1}^{t_2} \left[\int_V \delta \mathrm{U}^{\mathrm{T}} \mathrm{I} \ddot{\mathrm{U}} - \delta \mathrm{U}^{\mathrm{T}} \mathrm{E}_1^{\mathrm{T}} \mathrm{C} \mathrm{E}_1 \mathrm{U} - \delta \mathrm{U}^{\mathrm{T}} \mathrm{K}_{\mathrm{B}} \mathrm{U} \mathrm{d}V \right] \mathrm{d}t = 0 \qquad (12)$$

where U denotes the overall node displacement column vector with dimension $3NMP \times 1$, which is arranged as follows

$$\mathrm{U} = \left[\mathbf{u} \quad \mathbf{v} \quad \mathbf{w} \right]^{\mathrm{T}}$$
$$\mathbf{g} = \left[\mathbf{g}_1 \quad \mathbf{g}_2 \quad \cdots \quad \mathbf{g}_k \quad \cdots \quad \mathbf{g}_P \right]^{\mathrm{T}}, \mathbf{g} = \mathbf{u}, \mathbf{v}, \mathbf{w} \qquad (13)$$
$$\mathbf{g}_k = \left[\mathbf{g}_{1k} \quad \mathbf{g}_{2k} \quad \cdots \quad \mathbf{g}_{jk} \quad \cdots \quad \mathbf{g}_{Mk} \right]^{\mathrm{T}}$$
$$\mathbf{g}_{jk} = \left[\mathbf{g}_{1jk} \quad \mathbf{g}_{2jk} \quad \cdots \quad \mathbf{g}_{ijk} \quad \cdots \quad \mathbf{g}_{Njk} \right]^{\mathrm{T}}$$

The remaining matrices can be determined as

$$\mathrm{I} = \boldsymbol{\rho} \otimes \mathbf{I}_z \otimes \mathbf{I}_y \otimes \mathbf{I}_x, \boldsymbol{\rho} = \mathrm{diag}\left(\rho \quad \rho \quad \rho \right)$$
$$\mathrm{E}_1 = \begin{bmatrix} \mathbf{I}_z \otimes \mathbf{I}_y \otimes \mathbf{D}_x^{(1)} & \mathbf{0} & \mathbf{0} \\ \mathbf{0} & \mathbf{I}_z \otimes \mathbf{D}_y^{(1)} \otimes \mathbf{I}_x & \mathbf{0} \\ \mathbf{0} & \mathbf{0} & \mathbf{D}_z^{(1)} \otimes \mathbf{I}_y \otimes \mathbf{I}_x \\ \mathbf{I}_z \otimes \mathbf{D}_y^{(1)} \otimes \mathbf{I}_x & \mathbf{I}_z \otimes \mathbf{I}_y \otimes \mathbf{D}_x^{(1)} & \mathbf{0} \\ \mathbf{D}_z^{(1)} \otimes \mathbf{I}_y \otimes \mathbf{I}_x & \mathbf{0} & \mathbf{I}_z \otimes \mathbf{I}_y \otimes \mathbf{D}_x^{(1)} \\ \mathbf{0} & \mathbf{D}_z^{(1)} \otimes \mathbf{I}_y \otimes \mathbf{I}_x & \mathbf{I}_z \otimes \mathbf{D}_y^{(1)} \otimes \mathbf{I}_x \end{bmatrix} \qquad (14)$$
$$\mathrm{C} = \mathbf{C} \otimes \mathbf{I}_z \otimes \mathbf{I}_y \otimes \mathbf{I}_x =$$
$$\mathrm{K}_{\mathrm{B}} = \mathbf{k}_{\mathrm{B0}} \otimes \mathbf{I}_z \otimes \mathbf{I}_y \otimes \begin{bmatrix} 1 & 0 & \cdots & 0 \\ 0 & 0 & \cdots & 0 \\ \vdots & \vdots & \ddots & \vdots \\ 0 & 0 & \cdots & 0 \end{bmatrix}_{N \times N} + \mathbf{k}_{\mathrm{B1}} \otimes \mathbf{I}_z \otimes \mathbf{I}_y \otimes \begin{bmatrix} 0 & 0 & \cdots & 0 \\ 0 & 0 & \cdots & 0 \\ \vdots & \vdots & \ddots & \vdots \\ 0 & 0 & \cdots & 1 \end{bmatrix}_{N \times N}$$

in which the symbol $\otimes$ represents the Kronecker tensor product, $\mathbf{I}_x$, $\mathbf{I}_y$, $\mathbf{I}_z$ are identity tensor of N^{th}, M^{th}, P^{th} order, and $\mathbf{D}_x^{(1)}$, $\mathbf{D}_y^{(1)}$, $\mathbf{D}_z^{(1)}$ denote the matrices of differential weighting coefficients corresponding to the 1st order derivatives in the *x*-, *y*- and *z*- directions[42].

According to the DQM fundamentals, the triple integral of the function $f(x, y, z)$ over the domain of definition can be written as

$$\bullet \int_{z_1}^{z_P}\int_{y_1}^{y_M}\int_{x_1}^{x_N} f(x,y,z)\,\mathrm{d}x\mathrm{d}y\mathrm{d}z = \mathbf{C}_{03}\mathbf{f} \qquad (15)$$

where $\mathbf{f}$ denotes the column vector consisting of the function values of the function $f(x, y, z)$ at all nodes, and $\mathbf{C}_{03}$ is the $N\times M\times P$ dimensional diagonal matrix consisting of $N\times M\times P$ three-dimensional integrally weighted coefficients, with the specific expression referred to in ref.[42]. Then, Eq.(12) can be written as

$$\bullet\ \delta\mathrm{U}^{\mathrm{T}}\left(\mathbf{I}_{3\times3}\otimes\mathbf{C}_{03}\right)\mathrm{I}\ddot{\mathrm{U}} - \delta\mathrm{U}^{\mathrm{T}}\mathrm{E}_1^{\mathrm{T}}\left(\mathbf{I}_{6\times6}\otimes\mathbf{C}_{03}\right)\mathrm{C}\mathrm{E}_1\mathrm{U} - \delta\mathrm{U}^{\mathrm{T}}\left(\mathbf{I}_{3\times3}\otimes\mathbf{C}_{03}\right)\mathrm{K}_{\mathrm{B}}\mathrm{U}\mathrm{d}V = 0 \qquad (16)$$

The discretized governing equations of the three-dimensional fiber-plain-woven beam can be obtained by making $\delta\mathrm{U}^{\mathrm{T}} = 0$, $\mathrm{K} = \mathrm{E}_1^{\mathrm{T}}\left(\mathbf{I}_{6\times6}\otimes\mathbf{C}_{03}\right)\mathrm{C}\mathrm{E}_1 + \left(\mathbf{I}_{3\times3}\otimes\mathbf{C}_{03}\right)\mathrm{K}_{\mathrm{B}}$, $\mathrm{M} = \left(\mathbf{I}_{3\times3}\otimes\mathbf{C}_{03}\right)\mathrm{I}$

$$\bullet\ \mathrm{M}\ddot{\mathrm{U}} + \mathrm{K}\mathrm{U} = 0 \qquad (17)$$

Assuming $\mathrm{U} = \tilde{\mathrm{U}}e^{j\omega t}$, the modal problem of solving is converted to a matrix eigenvalue/eigenvector problem, which is solved directly to obtain the intrinsic frequency and modal shapes of the structure.

3. Results and discussion

A mathematical model for the vibration analysis of three-dimensional fiber-plain-woven beams is meticulously given in the last section and is applied in this section to predict the vibration behavior of 3D beams under general boundary conditions. In terms of the definition of the boundary conditions for a solid beam with stress-free side surfaces, several symbols are used to indicate the different boundary conditions at the end of $x=0$ or $x=L$, in which *F*, *S* and *C* are identified as the free, simply-supported as well as clamped boundary conditions. In addition, three elastic boundary conditions denoted by the symbols E_1, E_2 and E_3 are considered. Particularly, the values of spring stiffness corresponding to different boundary conditions are presented in Fig.3. Out of the convenience of explaining the physical insight into the vibration properties, an elastic 3D beam subjected to various boundary conditions is analyzed, and unless otherwise specified, its geometric parameters are defined as: H=0.25m, B/H=1, L/H=12. The beam material is assumed as a fiber-plain-woven reinforced resin matrix composite with the volume fraction of V_f= 0.28. The related material parameters(Including the elastic modulus, shear modulus, Poisson's ratio, density.) corresponding to different volume fractions are shown in Fig.2.

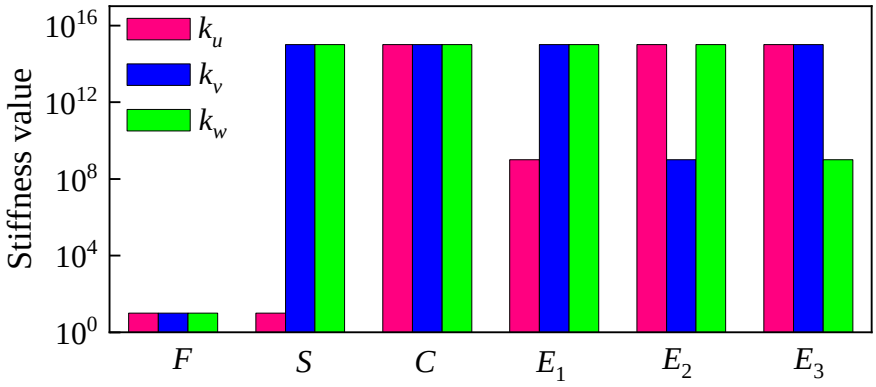

Figure 3: Detail stiffness values for different boundary conditions

In order to clarify the accuracy of the developed beam model and to demonstrate its applicability, several test examples are provided for the free vibration problem of a 3D beam. The solutions calculated by the present formulation are compared with theoretical solutions published in the literature as well as finite element numerical results. As the first case, a thick isotropic beam under S-S boundary conditions is employed. The related calculation parameters for the present analysis are listed as: B=H=0.1m and L/H=10 for geometric dimensions; E=210 GPa, μ=0.167 and ρ=7800kg/m^3 for material properties. Table 2 lists the first eight frequency parameters Ω for a S-S isotropic beam. Note that the flexural modes in the *xy*- and *xz*-planes are the same since the beam has a square cross-section, and thus only the flexural modes in the *xy*-plane are involved. In addition, the 2D exact results reported by Chen et al.[43], the 3D elastic solutions obtained by Qu et al.[29] based on a modified variational principle, and the finite element solutions[29] computed using Ansys Software are also provided in Table 2 for comparative purposes. Of note, the first frequency corresponding to the rigid motion is close to zero and is not included in Table 2. In general, the present results are in good agreement with the given reference solutions. Also, the theoretical solutions obtained from the present methodology are slightly higher than those reported by Chen et al.[43]. Particularly, it should be pointed out that all vibration modes of a beam can be examined by the current three-dimensional elastic formulation, whereas the two-dimensional theory allows the calculation of accurate results only for bending, longitudinal, thickness torsion and shear modes.

Table 1: Comparison of the first eight frequency parameters $\Omega = \omega H\sqrt{\rho / G_{12}}$ for a S-S beam (L=1, B=H=0.1m)

Source	Mode order							
	1	2	3	4	5	6	7	8
Qu et al.[29]	0.042874	0.16445	0.28698	0.34817	0.47984	0.57395	0.57613	0.83384
Chen et al.[43]	0.042878	0.16451	--	0.34841	0.47990	--	0.57675	0.83507
Ansys[29]	0.042875	0.16447	0.28736	0.34824	0.47984	0.57470	0.57631	0.83420
Present	0.042879	0.16452	0.28852	0.34846	0.47984	0.57686	0.57701	0.83527

In what follows, a comparison case related to the first eight frequency for a F-F composite beam is given in Table 2. The calculation parameters is defined as: (a) E_{11}=37.41 GPa, E_{22}=E_{33}=13.67 GPa, G_{12}=5.478 GPa, G_{13}=6.03 GPa, G_{23}=6.666 GPa, μ_{12} =μ_{12} =μ_{23}=0.3 for material properties; (b) L=0.21008 m, B=1.696×10^{-2}m, H=3.33×10^{-3}m for geometric dimensions. The reference solutions used for comparison include: three-dimensional elasticity solutions reported by Qu et al.[29], the experimental data provided by Ritchie et al.[44] as well as Ansys results. As s observed in Table 2, the present solutions can well match with the reference data obtained by different method.

Table 2: Comparison of the first eight frequency for a F-F composite beam (L=0.21008 m, B=1.696×10^{-2}m, H=3.33×10^{-3}m)

Source	Mode order							
	1	2	3	4	5	6	7	8
Qu et al.[29]	337.09	926.51	1439.78	1654.61	1808.42	2910.6	2971.84	4231.79
Ritchie et al.[44]	337.7	926.7	1434.8	--	1812.3	--	2979.1	--
Ansys[29]	337.10	926.69	1441.05	1654.72	1809.16	2913.27	2973.91	4232.79
Present	337.62	927.99	1442.00	1657.25	1811.31	2915.26	2976.58	4238.56

To further present the accuracy of the present method, Table 3 shows the first ten values of natural frequencies for a 3D thick fiber-plain-woven beams with various boundary conditions, in which three types of boundary conditions are included, i.e., F-F, C-F and C-C. Here, the finite element model of the 3D beam has been constructed by employing the C3D8R solid elements, and the 3D FEM solutions obtained

from commercial Abaqus software are presented for illustrating validity. Of note, the first six natural frequencies are essentially zero for the F-F case, which corresponds to the rigid displacements of the beams and is therefore ignored in the table. The results in Table 3 make it clear that the results are in good agreement with the ones calculated from finite element numerical simulation, and the maximum relative error is not more than 0.3%, which demonstrates the excellent numerical potential of this method to analyze the vibration behaviors of the 3D fiber-plain-woven beam. It is worth mentioning that, although the beam used in this example has a square cross-section, the vibration frequencies corresponding to the flexible modes (such as f_1, f_2 in Table 3) are different in the *xy*- and *xz*-planes due to the fact that the material parameters are different in the *y*- and *z*-directions, which is significantly different from the vibration frequencies of isotropic beams having a square cross-section.

Table 3: First ten natural frequencies (Hz) of 3D fiber-plain-woven beams with different boundary constraints (*L*=3, *B*=0.25m, *H*=0.25m)

Mode order	F-F			C-F			C-C		
	FEM	Present	diff.%	FEM	Present	diff.%	FEM	Present	diff.%
f_1	130.20	130.32	-0.09	21.531	21.554	-0.11	112.28	112.37	-0.08
f_2	132.28	132.41	-0.10	21.685	21.708	-0.11	118.11	118.19	-0.07
f_3	197.41	197.77	-0.18	99.137	99.33	-0.19	199.34	199.73	-0.20
f_4	308.49	308.74	-0.08	117.61	117.70	-0.08	258.35	258.47	-0.05
f_5	322.80	323.08	-0.09	122.00	122.10	-0.08	279.18	279.28	-0.04
f_6	395.49	396.27	-0.20	281.92	282.09	-0.06	399.24	400.07	-0.21
f_7	512.85	513.25	-0.08	297.74	298.33	-0.20	432.49	432.67	-0.04
f_8	550.28	550.73	-0.08	299.86	300.04	-0.06	474.76	474.90	-0.03
f_9	594.71	596.04	-0.22	411.19	411.24	-0.01	600.09	601.47	-0.23
f_{10}	721.68	722.35	-0.09	470.03	470.27	-0.05	619.92	620.24	-0.05

According to the theoretical modeling in the previous section, the vibration frequencies depend on the spring stiffness at the beam boundary. For this reason, Fig.4 investigates the effect of variation of the stiffness value of the boundary spring on the first four orders of vibration frequency of 3D fiber-plain-woven beam. It should be pointed out that, in order to facilitate the analysis of the effect of a particular stiffness parameter on the vibration frequency, it is maintained that this parameter is varied from 10 to 10^{17} at both ends of the beam, while others are set to 10^{16}. For instance, to investigate the effect of k_u, it is assumed that the parameter k_u is increased from 10 to 10^{17}, while k_v=k_w=10^{16} are employed. From Fig. 4, it can be observed that, the frequency parameter increases rapidly with the increase of all the constraint parameters within a certain range. And beyond this range, the frequency changes are relatively very little. Additionally, it can also be found that there are differences in the sensitivity of the natural frequencies corresponding to different modal orders to the boundary springs. For example, in the case study of k_u, the parameter sensitivity interval corresponding to the first-order frequency (namely, f_1) is at [10^5,10^{13}], while the one of the second-order frequency are approximately in the interval of [10^8, 10^{13}]. Another noteworthy phenomenon is that the parameters k_v and k_w have similarity in the pattern of influence and sensitivity intervals of vibration frequencies, but there are some differences with those of k_u. Based on the above analysis, the effect of spring stiffness on the natural frequencies of the fiber-plain-woven 3D beam is classified into the free, elastic and clamped constraints. Therefore, the general boundary conditions can be obtained by setting a reasonable boundary stiffness. This justifies the setting of the boundary conditions in Fig. 3.

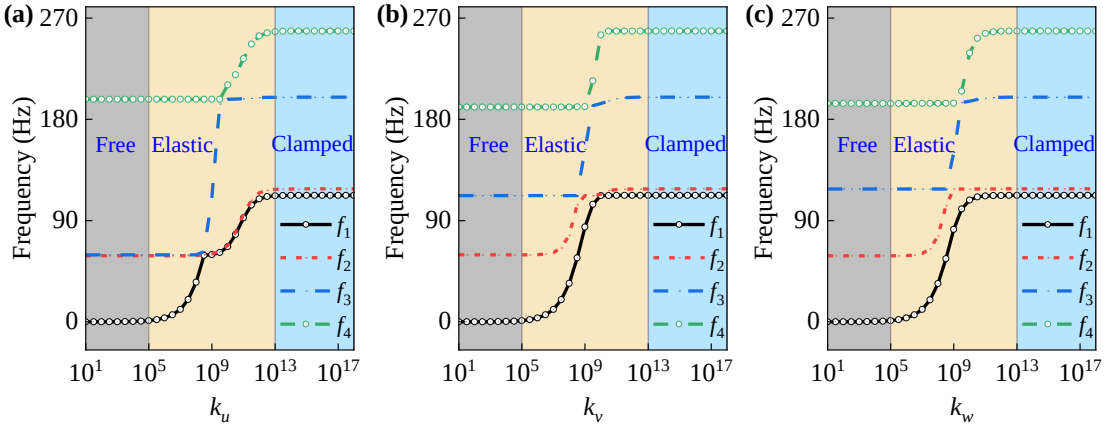

Figure 4: Effect of boundary stiffness on the natural frequency of a 3D fiber-plain-woven 3D beam: (a) k_u; (b) k_v; (c) k_w.

To further deepen our knowledge of the vibration behaviors of the fiber-plain-woven 3D beam, some mode shapes of 3D fiber-plain-woven beam with different boundary stiffness are displayed in Table 4. After solving the eigenvalue problem in Eq. (17), these mode shapes are plotted in the 3D view by employing the Eq. (13). Of note, since the spring stiffness is small (e.g., k_u=10), the first-order mode shape is rigid mode, which are ignored here. There are torsional modes in the figure (e.g., f_4 for k_u = 10, 10^9) that cannot be considered by employing the one-dimensional simplified beam theory, while others are bending motions in the *xz*- or *xy*-planes.

Table 4: Mode shapes of 3D fiber-plain-woven beam with different boundary stiffness

Type	Value	f_1	f_2	f_3	f_4
k_u	10^1	--			
	10^9				
	10^{16}				
k_v	10^1	--			
	10^9				
	10^{16}				
k_w	10^1	--			

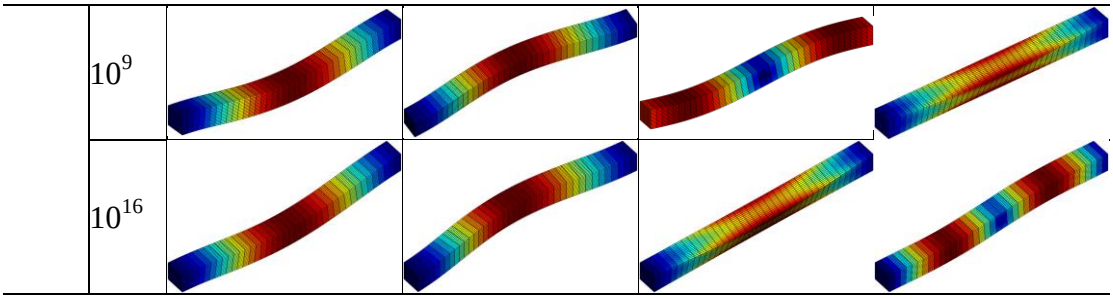

Fig.5 shows effect of the fiber volume fraction V_f on the first four natural frequencies of 3D fiber-plain-woven beam. Here, C-C and C-F boundary conditions are involved for the current study. According to the results in Fig.5, when V_f is increased from 0.28 to 0.42, the other material parameters (i.e., Young's modulus, shear modulus, and density) are subsequently increased, except for the Poisson's ratio of the fiber-plain-woven material, which is slightly decreased. The synergistic change in the above material parameters resulted in an increase in the overall stiffness-mass ratio of the fiber-plain-woven 3D beam, which leads to an approximately linear increase in the vibration frequencies of the beam. In addition, it can also be observed that the difference in frequency between f_1 and f_2 is significant in the C-C case, while the difference in the variation curves is relatively small for C-F case. This is due to the fact that the smaller the boundary stiffness makes the system less stiffness, and thus the material anisotropy has less effect on the different order frequencies of the 3D beam.

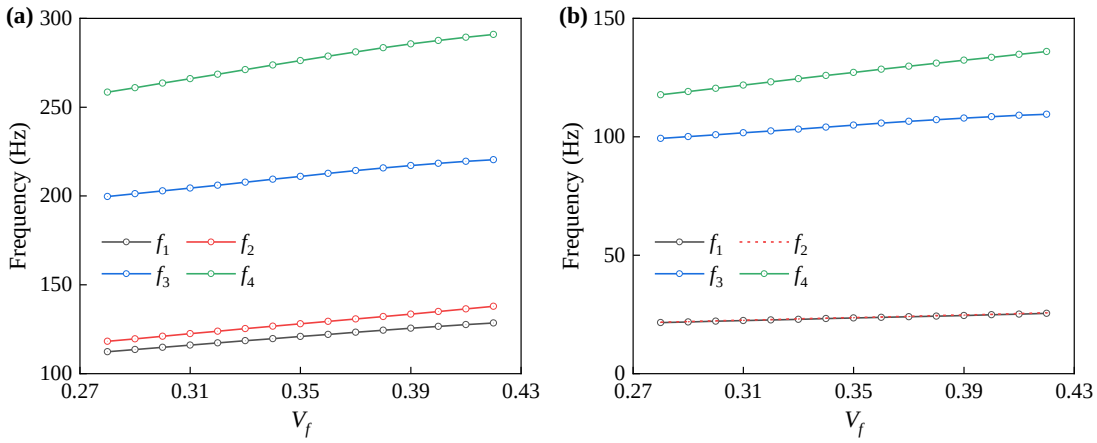

Figure 5: Effect of the fiber volume fraction V_f on the first four natural frequencies of 3D fiber-plain-woven beam: (a) C-C; (b) C-F.

Fig.6 shows the variation of the fundamental frequency of 3D fiber-plain-woven beam with its width and thickness, where four classical boundary conditions (*i.e.*, F-F, C-F, C-C, S-S.) are considered. Here, the thickness and width of the beam are assumed to vary from 0.05m to 1m and the length L is kept constant. It can be found from Fig. 6 that, regardless of the boundary conditions, the fundamental frequency of the beam always increases due to the increase in the stiffness-to-mass ratio of the structure as a result of the increase in the width or thickness of the beam. Table 5 gives the fundamental frequencies for 3D fiber-plain-woven beam with different boundary conditions subjected to various boundary conditions and different ratio of L/H. From the tables, it can be found that, as the ratio of L/H and the parameter V_f increase, the fundamental frequency shows an increasing trend. Also, there is a significant difference in the fundamental frequency of the beams when the boundary conditions are different, which indicates that the structural vibration frequency is sensitive to the boundary conditions. In view of the fact that there is no available literature published on the free vibration properties of fiber-plain-woven 3D beams, these new data can be employed as the benchmark solutions for checking the accuracy of other simplified beam theories.

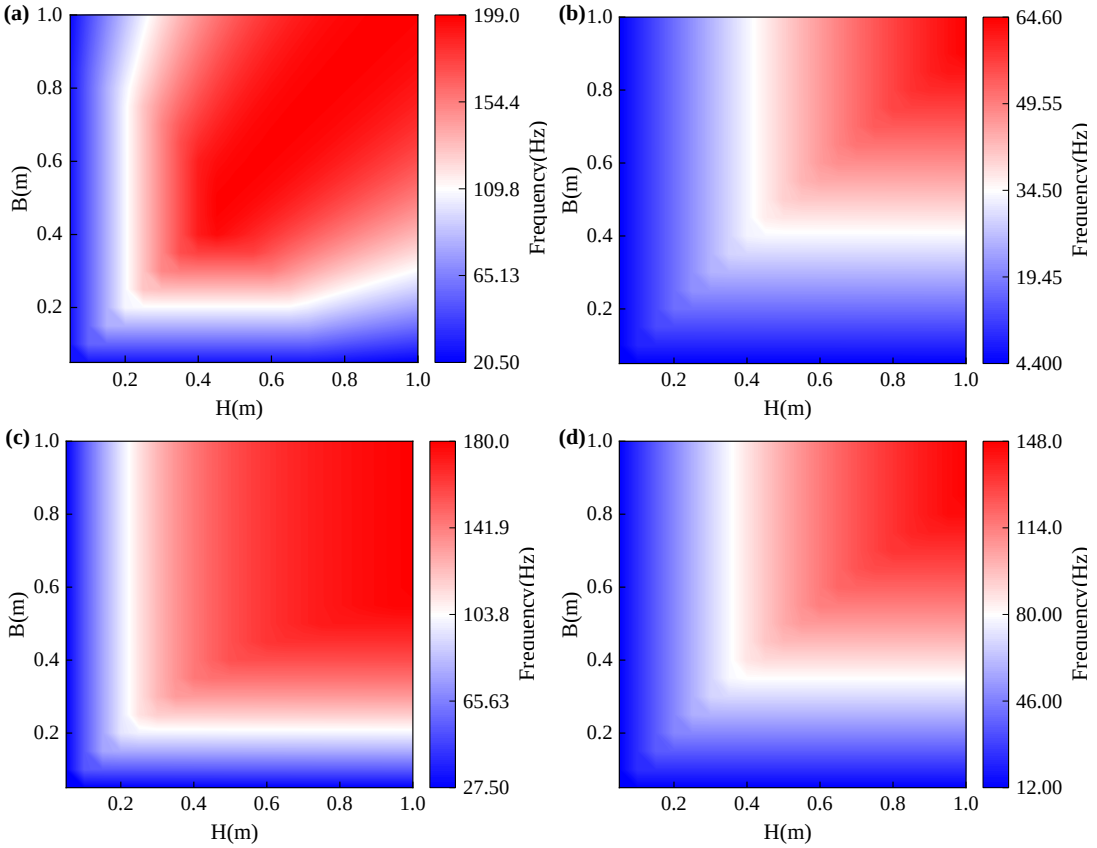

Figure 6: Effect of thickness and length on the fundamental frequency of 3D fiber-plain-woven beam: (a) F-F; (b) C-F; (c) C-C; (d) S-S.

Table 5: The fundamental frequency for 3D fiber-plain-woven beam with different boundary conditions(B/H=2)

L/*H*	V_f	Boundary condition							
		C-C	C-F	F-F	S-S	C-S	E_1-E_1	E_2-E_2	E_3-E_3
2	0.28	1122.7	462.01	918.14	996.10	1144.3	272.93	268.78	266.87
	0.36	1191.0	495.83	980.61	1063.6	1217.9	268.60	265.15	263.42
	0.42	1221.5	514.61	1021.4	1098.3	1257.8	265.48	262.45	260.69
4	0.28	516.67	162.82	496.67	390.91	551.15	192.75	186.51	183.05
	0.36	550.56	177.25	530.55	422.51	587.76	189.74	184.55	181.50
	0.42	567.32	186.91	552.95	442.14	609.22	187.56	183.01	180.00
6	0.28	311.98	80.15	334.62	204.86	358.32	157.18	149.01	143.48
	0.36	334.32	87.84	357.46	223.24	382.52	154.77	147.96	143.17
	0.42	346.53	93.34	372.59	235.77	397.31	153.02	147.04	142.46

4. Concluding remarks

This study investigates the free vibration behaviors of a fiber-plain-woven 3D beam under various BCs, using a numerical modeling method based on three-dimensional linear elasticity theory and the differential quadrature approach. The vibration equations are derived using 3D theory, incorporating the DQM, where arbitrary boundary conditions are achieved by means of boundary springs with variable stiffness. The validity of the proposed model is verified by comparing the free vibration frequencies of the developed isotropic and composite beam model with the reported literature solutions and finite element simulation data. Subsequently, some key parameters (such as boundary stiffness, volume fraction etc.) are employed to investigate the influence of these parameters on the vibration behaviors of 3D fiber-plain-woven beam. From the current investigations, some findings can be concluded as follows: The variation of the stiffness value of the

boundary spring in a certain interval has a significant effect on the vibration frequency of the three-dimensional beam, and there is a significant difference between the sensitivity intervals of different orders of vibration frequency to the boundary stiffness; Additionally, the structural geometrical parameters also play an important role, since these factors can change the structural stiffness-to-mass ratio, which in turn makes the modal frequencies change. Furthermore, increasing the total fiber volume fraction V_f enhances the natural frequencies to avoid low frequency resonance. Also, the theoretical model developed in the current investigation can be employed as an effective tool in the dynamic analysis and design of beam structures.

References

1. M. Aydogdu, Vibration analysis of cross-ply laminated beams with general boundary conditions by Ritz method, International Journal of Mechanical Sciences, 47 (2005) 1740-1755.
2. M. Aydogdu, Free vibration analysis of angle-ply laminated beams with general boundary conditions, Journal of reinforced plastics and composites, 25 (2006) 1571-1583.
3. J.-M. Berthelot, Damping analysis of laminated beams and plates using the Ritz method, Composite Structures, 74 (2006) 186-201.
4. O.A. Bauchau, S. Han, A. Mikkola, M.K. Matikainen, P. Gruber, Experimental validation of flexible multibody dynamics beam formulations, Multibody System Dynamics, 34 (2015) 373-389.
5. J.M. Ramirez, C.D. Gatti, S.P. Machado, M. Febbo, An experimentally validated finite element formulation for modeling 3D rotational energy harvesters, Engineering Structures, 153 (2017) 136-145.
6. H. Farokhi, Y. Xia, A. Erturk, Experimentally validated geometrically exact model for extreme nonlinear motions of cantilevers, Nonlinear dynamics, 107 (2022) 457-475.
7. L.F. Hussein, M.M. Khattab, M.S. Farman, Experimental and finite element studies on the behavior of hybrid reinforced concrete beams, Case Studies in Construction Materials, 15 (2021) e00607.
8. T.-N. Le, J.-M. Battini, M. Hjiaj, A New Corotational Element for Nonlinear Dynamic Analysis of 3D Beams, pp. 3586-3608.
9. P.-T. Pham, Q.C. Nguyen, M. Yoon, K.-S. Hong, Vibration control of a nonlinear cantilever beam operating in the 3D space, Scientific Reports, 12 (2022) 13811.
10. G. Wang, Z. Qi, J. Xu, A high-precision co-rotational formulation of 3D beam elements for dynamic analysis of flexible multibody systems, Computer Methods in Applied Mechanics and Engineering, 360 (2020) 112701.
11. E. Yıldırım, N. Aktürk, Dynamic modeling and nonlinear free vibration analysis of a rotating 3D beam induced by adjacent two revolute joints, Multibody System Dynamics, 59 (2023) 429-446.
12. E. Zupan, D. Zupan, Dynamic analysis of geometrically non-linear three-dimensional beams under moving mass, Journal of Sound and Vibration, 413 (2018) 354-367.
13. K. Ordaz-Hernandez, X. Fischer, Fast reduced model of non-linear dynamic Euler–Bernoulli beam behaviour, International Journal of Mechanical Sciences, 50 (2008) 1237-1246.
14. Y. Shen, A. Vizzaccaro, N. Kesmia, T. Yu, L. Salles, O. Thomas, C. Touzé, Comparison of reduction methods for finite element geometrically nonlinear beam structures, Vibration, 4 (2021) 175-204.
15. B. Wang, Y. Li, P. Hao, Y. Zhou, Y. Zhao, B. Wang, Free vibration analysis of beam-type structures based on novel reduced-order model, AIAA Journal, 55 (2017) 3143-3152.
16. C. Yang, K. Liang, Y. Rong, Q. Sun, A hybrid reduced-order modeling technique for nonlinear structural dynamic simulation, Aerospace Science and Technology, 84 (2019) 724-733.
17. W. Fang, T. Yu, T.Q. Bui, Analysis of thick porous beams by a quasi-3D theory and isogeometric analysis, Composite Structures, 221 (2019) 110890.
18. H. Hu, T. Yu, T.Q. Bui, Dynamic and static isogeometric analysis for laminated Timoshenko curved microbeams, Engineering Analysis with Boundary Elements, 128 (2021) 90-104.
19. E. Shafei, S. Faroughi, A. Reali, Geometrically nonlinear vibration of anisotropic composite beams using isogeometric third-order shear deformation theory, Composite Structures, 252 (2020) 112627.
20. I.N. Tsiptsis, E.J. Sapountzakis, Isogeometric analysis for the dynamic problem of curved structures including warping effects, Mechanics Based Design of Structures and Machines, 46 (2018) 66-84.

21. O. Weeger, B. Narayanan, M.L. Dunn, Isogeo metric shape optimization of nonlinear, curved 3D beams and beam structures, Computer Met hods in Applied Mechanics and Engineering, 3 45 (2019) 26-51.
22. O. Weeger, U. Wever, B. Simeon, Isogeometri c analysis of nonlinear Euler–Bernoulli beam vibrations, Nonlinear Dynamics, 72 (2013) 81 3-835.
23. O. Weeger, S.-K. Yeung, M.L. Dunn, Fully iso geometric modeling and analysis of nonlinear 3D beams with spatially varying geometric an d material parameters, Computer methods in a pplied mechanics and engineering, 342 (2018) 95-115.
24. G. Zhang, R. Alberdi, K. Khandelwal, Analysi s of three-dimensional curved beams using iso geometric approach, Engineering Structures, 1 17 (2016) 560-574.
25. J.B. Jonker, Three-dimensional beam element for pre-and post-buckling analysis of thin-wall ed beams in multibody systems, Multibody sy stem dynamics, 52 (2021) 59-93.
26. C.T. Nguyen, S. Oterkus, Peridynamics for ge ometrically nonlinear analysis of three-dimens ional beam structures, Engineering Analysis w ith Boundary Elements, 126 (2021) 68-92.
27. Y.H. Huang, Z.G. Zhang, Y.X. Peng, H.X. Hu a, A three-dimensional beam formulation for l arge deformation and an accurate implementat ion of the free boundary, International Journal of Non-Linear Mechanics, 134 (2021) 103736.
28. V.X. Nguyen, K.T. Nguyen, S. Thai, Large def lection analysis of functionally graded beams based on geometrically exact three-dimension al beam theory and isogeometric analysis, Inte rnational Journal of Non-Linear Mechanics, 1 46 (2022) 104152.
29. Y. Qu, G. Yuan, S. Wu, G. Meng, Three-dimen sional elasticity solution for vibration analysis of composite rectangular parallelepipeds, Euro pean Journal of Mechanics - A/Solids, 42 (201 3) 376-394.
30. M. Chen, G. Jin, Y. Zhang, F. Niu, Z. Liu, Thr ee-dimensional vibration analysis of beams wi th axial functionally graded materials and vari able thickness, Composite Structures, 207 (20 19) 304-322.
31. Z. Gao, L. Chen, A review of multi-scale num erical modeling of three-dimensional woven fa bric, Composite Structures, 263(2021)113685.
32. G. Nicoletto, E. Riva, Failure mechanisms in t will-weave laminates: FEM predictions vs. ex periments, Composites Part A: applied science and manufacturing, 35 (2004) 787-795.
33. X. Liu, K. Rouf, B. Peng, W. Yu, Two-step ho mogenization of textile composites using mec hanics of structure genome, Composite Structu res, 171 (2017) 252-262.
34. X. Liu, W. Yu, F. Gasco, J. Goodsell, A unified approach for thermoelastic constitutive modeli ng of composite structures, Composites Part B: Engineering, 172 (2019) 649-659.
35. A. Adumitroaie, E.J. Barbero, Beyond plain w eave fabrics–II. Mechanical properties, Comp osite Structures, 93 (2011) 1449-1462.
36. H. Zhang, M. Shen, T. Liu, Z. Li, Q. Wang, D ynamic Modeling and Vibration Characteristic Analysis of Fiber Woven Composite Shaft–Di sk Rotor with Weight-Reducing Holes, Applie d Sciences (2076-3417), 14 (2024).
37. P. Tan, L. Tong, G.P. Steven, A flexible 3D FE A modeling approach for predicting the mecha nical properties of plain weave unit cell, 1997, pp. 67-76.
38. P. Tan, L. Tong, G.P. Steven, A three-dimensio nal modelling technique for predicting the line ar elastic property of opened-packing woven f abric unit cells, Composite structures, 38 (199 7) 261-271.
39. P. Tan, L. Tong, G.P. Steven, Micromechanics models for the elastic constants and failure str engths of plain weave composites, Composite structures, 47 (1999) 797-804.
40. Y.C. Zhang, J. Harding, A numerical microme chanics analysis of the mechanical properties of a plain weave composite, Computers & Stru ctures, 36 (1990) 839-844.
41. Q. Huang, Y. Gao, F. Hua, W. Fu, Q. You, J. G ao, X. Zhou, Free vibration analysis of carbon-fiber plain woven reinforced composite conica l-cylindrical shell under thermal environment with general boundary conditions, Composite Structures, 322 (2023) 117340.
42. R. Ansari, M.F. Shojaei, A. Shahabodini, M. B azdid-Vahdati, Three-dimensional bending and vibration analysis of functionally graded nano plates by a novel differential quadrature-based approach, Composite Structures, 131 (2015) 7 53-764.
43. W.Q. Chen, C.F. Lü, Z.G. Bian, A semi-analyti cal method for free vibration of straight orthot ropic beams with rectangular cross-sections, Mechanics Research Communications, 31 (20

04) 725-734.
44. I.G. Ritchie, H.E. Rosinger, A.J. Shillinglaw, W.H. Fleury, The dynamic elastic behaviour of a fibre-reinforced composite sheet. I. The precise experimental determination of the principal elastic moduli, Journal of Physics D: Applied Physics, 8 (1975) 1733.